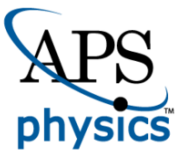

Complete Quantum Coherent Control of Ultracold Molecular Collisions

Adrien Devolder, Paul Brumer, and Timur V. Tscherbul

Phys. Rev. Lett. **126**, 153403 — Published 13 April 2021

DOI: 10.1103/PhysRevLett.126.153403

Complete quantum coherent control of ultracold molecular collisions

Adrien Devolder[1], Paul Brumer[1], and Timur V. Tscherbul[2]
[1] *Chemical Physics Theory Group, Department of Chemistry, and Center for Quantum Information and Quantum Control, University of Toronto, Toronto, Ontario, M5S 3H6, Canada*
[2] *Department of Physics, University of Nevada, Reno, NV, 89557, USA*
(Dated: March 22, 2021)

We show that quantum interference-based coherent control is a highly efficient tool for tuning ultracold molecular collision dynamics, and is free from the limitations of commonly used methods that rely on external electromagnetic fields. By varying the relative populations and phases of initial coherent superpositions of degenerate molecular states, we demonstrate complete coherent control over integral scattering cross sections in the ultracold s-wave regime of both the initial and final collision channels. The proposed control methodology is applied to ultracold O_2 + O_2 collisions, showing extensive control over s-wave spin-exchange cross sections and product branching ratios over many orders of magnitude.

Introduction. Recent advances in experimental techniques for cooling and trapping neutral atoms and polar molecules [1–4] have reignited interest in novel approaches to controlling atomic and molecular collisions and chemical reactivity at ultralow temperatures. Such approaches are central to using ultracold atoms and molecules in optical lattices as a platform for quantum information processing and quantum simulation [1, 5–7] and to studying exotic regimes of ultracold controlled chemistry [1, 8, 9]. The vast majority of control scenarios developed thus far for ultracold atomic and molecular collisions are based on a combination of static (dc) and time-varying (ac) external electromagnetic fields. Examples include magnetic and optical Feshbach resonances [10–15], electric field-induced resonances [16, 17], microwave dressing [18–24], parity breaking in superimposed electric and magnetic fields [25, 26], and low-dimensional confinement [27–29].

Despite the success of these control methods, they suffer from a number of serious limitations. First, dc fields control cannot be applied to control molecular systems that lack magnetic (or electric) dipole moments, such as H_2. Such systems are often of great chemical and astrochemical interest, and have been studied with unprecedented theoretical accuracy, such as the archetypal chemical reaction F + H_2 → HF + H [30–32]. Second, the extent of control is limited by the magnitude of molecular Stark and Zeeman shifts induced by practical laboratory dc fields. Finally, the presence of external field-induced perturbations can be counterproductive in high-precision experiments, such as those involving optical lattice clocks [33].

Quantum coherent control is a well-established approach free of these limitations, whereby quantum interference of transition pathways from an initially prepared coherent superposition of molecular states is used to maximize or minimize the transition amplitudes[34, 35]. While coherent control has enjoyed great success when applied to unimolecular processes (such as photodissociation), its application to bimolecular collision dynamics has been limited by large uncontrollable incoherent terms, to symmetry reasons [36, 37] or the need to entangle the internal and external degrees of freedom of collision partners, a significant experimental challenge [34, 38, 39] that can be circumvented by using superpositions of *degenerate* magnetic sublevels (m-superpositions) as initial scattering states [36, 37, 40].

Here, we recognize quantum coherent control [34–39, 41] as an important approach to manipulating ultracold molecular collisions with an efficiency exceeding that of their traditional dc counterparts. We show that by forming coherent superpositions of initial molecular states, it is possible to achieve complete control over integral scattering cross sections and branching ratios in the s-wave regime of both the initial and final collision channels (the double s-wave regime). Using rigorous quantum scattering calculations [42] we demonstrate extensive control of ultracold O_2 + O_2 collisions, a system recently observed experimentally in a magnetic trap [43], over the unprecedented range of ten orders of magnitude. Our coherent control scenario does not require external electromagnetic fields and can be applied to a wide range of atomic and molecular collisions that are not amenable to external dc field control, such as those involving H_2 [39] and homonuclear alkali-metal dimers. This significantly expands the toolbox of methods for manipulating ultracold molecular collisions.

Theory. As a first step to achieving coherent control of cold collisions, we prepare an initial coherent superposition of N_s two-molecule internal states $|a_i b_i\rangle$, where a_i and b_i denote internal states of each of the two colliding molecules:

$$|\psi_s\rangle = \sum_{i=1}^{N_s} c_i \, |a_i b_i\rangle \, . \tag{1}$$

Using the standard expression for the state-to-state integral cross section (ICS) $\sigma_{ab\to a'b'} = \frac{\pi}{k^2}\sum_{\ell,m_\ell}\sum_{\ell',m'_\ell}|T_{ab\ell,m_\ell\to a'b'\ell'm'_\ell}|^2$, where ℓ and ℓ' are the initial and final orbital angular momenta of the collision, m_ℓ and m'_ℓ are the initial and final projections of ℓ and ℓ' on the space-fixed quantization axis Z, k is the initial relative momentum, and $T_{ab\ell m_\ell\to a'b'\ell'm'_\ell}$ are the T-matrix elements, we obtain the cross-section for

scattering from the initial superposition (1) to the final two-molecule internal state $|a'b'\rangle$ as

$$\sigma_{s\to a'b'} = \frac{\pi}{k^2}\sum_{\ell,m_\ell}\sum_{\ell',m'_\ell}\left|\sum_{i=1}^{N_s} c_i T_{a_i b_i \ell m_\ell \to a'b'\ell' m'_\ell}\right|^2 . \quad (2)$$

Because there is no interference between the terms with different ℓ, m_ℓ, ℓ', and m'_ℓ in Eq. (2), the efficiency of coherent control of the ICS depends on how well we can control the individual partial wave contributions. Thus, we expect the control efficiency to be strongly enhanced at low temperatures, when only a limited number of initial and final partial wave terms are present in Eq. (2). In particular, in the limit of zero collision energy, only s-wave terms with $\ell = 0, m_\ell = 0$ contribute to the ICS due to the Wigner threshold law [44, 45], and the number of partial waves in the final channel is often strongly limited by angular momentum conservation [46, 47]. This leads us to expect a large extent of coherent control of nearly thermoneutral collisions dominated by s-waves in both the incident and final scattering channels, such as spin-exchange atomic and molecular collisions considered here, Förster resonant collisions of Rydberg atoms [48–53], atom-dimer exchange chemical reactions [54], excitation exchange between identical atoms or molecules [55], charge transfer in cold ion-atom collisions [56–58], and rotational angular momentum projection-changing collisions, e.g., $H_2(j = 1, m = 1) + H_2(j = 1, m = -1) \to 2H_2(j = 1, m = 0)$].

Consider then a coherent superposition of two incident s-wave channels $|a_1b_100\rangle$ and $|a_2b_200\rangle$, which allows for coherent control of the ICS to the final s-wave channel $|a'b'00\rangle$. Note that the two channels must correspond to the same combined angular momentum projection $M_{ab} = m_{a_1} + m_{b_1} = m_{a_2} + m_{b_2}$ [36]. Superpositions of states with different M_{ab} (i.e. $m_{a_1} + m_{b_1} \neq m_{a_2} + m_{b_2}$) only allow for a limited control of differential cross sections resolved over the scattering angles θ and ϕ [37]. It also the reason that no coherent control was observed in cold m-changing collisions of H_2 isotopes [59–62]. This work is free from such limitations. We stress that while the theory outlined below is developed for s-wave collisions, it is equally applicable to the partial wave-resolved ICSs for any given (ℓ, m_ℓ) and (ℓ', m'_ℓ).

In the s-wave scattering case, Eq. (2) reduces to

$$\sigma_{s\to a'b'} = \frac{\pi}{k^2}\left|\cos\eta T_1 + \sin\eta e^{i\beta} T_2\right|^2 , \quad (3)$$

where we define $c_1 = \cos\eta$, $c_2 = \sin\eta e^{i\beta}$, $T_1 = T_{a_1b_100\to a'b'00}$ and $T_2 = T_{a_2b_200\to a'b'00}$. Note that η defines the relative population of each state in the superposition while β gives the relative phase between the states.

The values of c_1 and c_2 that extremize the ICS can be found by diagonalizing the matrix $\mathcal{T}_{ij} = T_i T_j^*$ [63]. The lowest eigenvalue corresponds to $\sigma^{\min}_{s\to a'b'} = 0$, which shows that *it is always possible to coherently suppress collision-induced transitions to any given final channel* $|a'b'00\rangle$ regardless of the values of T_1 and T_2. The optimal values of the superposition parameters η and β that minimize the ICS are given by

$$\eta_{\min} = \cos^{-1}\left[\sqrt{\sigma_2/(\sigma_1+\sigma_2)}\right] = \tan^{-1}(\sqrt{\sigma_1/\sigma_2}) \quad (4)$$

$$\beta_{\min} = (\delta_2 - \delta_1) - \pi, \quad (5)$$

where $\sigma_1 = \frac{\pi}{k^2}|T_1|^2$ and $\sigma_2 = \frac{\pi}{k^2}|T_2|^2$ are the s-wave ICS for the incident channels $|a_1b_100\rangle$ and $|a_2b_200\rangle$.

From the second eigenvalue of $\mathcal{T}_{ij}$, we obtain the maximum value of the ICS, which is given by the sum of the ICSs from the initial channels $|a_1b_100\rangle$ and $|a_2b_200\rangle$

$$\sigma^{\max}_{s\to a'b'} = \sigma_1 + \sigma_2. \quad (6)$$

Using coherent control, it is therefore possible to tune the s-wave ICSs between zero and $\sigma_1 + \sigma_2$. As σ_1 and σ_2 can reach very large values near collision thresholds [9, 44, 45] a very wide control range is possible, as shown below for $O_2 + O_2$ collisions. The superposition angles η and β that maximize the ICS are given by

$$\eta_{\max} = \cos^{-1}\left[\sqrt{\sigma_1/(\sigma_1+\sigma_2)}\right] = \tan^{-1}(\sqrt{\sigma_2/\sigma_1}) \quad (7)$$

$$\beta_{\max} = \delta_2 - \delta_1. \quad (8)$$

Interestingly, the values of the superposition parameters that minimize and maximize the ICS are related by $\eta_{\max} + \eta_{\min} = \pi/2$ and $\beta_{\max} - \beta_{\min} = \pi$. We note that while knowledge of the ICS suffices to determine the optimal values of η, this is not the case for $\beta_{\min}$ and $\beta_{\max}$, which require knowledge of the phases of S-matrix elements. Thus, measurements of the ICSs of molecules in known initial superpositions can be used to infer complete amplitude and phase information about the S-matrix elements. Indeed, this is a general characteristic of many coherent control scenarios [34].

Having demonstrated complete coherent control of the total ICS, we now show that such control can be extended to include the branching ratios $\sigma_{s\to 1'}/\sigma_{s\to 2'}$ for transitions to the final channels $|1'\rangle = |a'_1b'_100\rangle$ and $|2'\rangle = |a'_2b'_200\rangle$. As shown above, there exists a superposition, defined by the parameters $\eta^{1'}_{\min}$ and $\beta^{1'}_{\min}$, for which the s-wave ICS $\sigma_{s\to 1'}$ vanishes. Similarly, there is a superposition with the parameters $\eta^{2'}_{\min}$ and $\beta^{2'}_{\min}$, for which the ICS $\sigma_{s\to 2'}$ vanishes. Then, the ICS ratio $\sigma_{s\to 1'}/\sigma_{s\to 2'}$ can be varied from zero to infinity by tuning the superposition parameters from $(\eta^{1'}_{\min},\ \beta^{1'}_{\min})$ to $(\eta^{2'}_{\min},\ \beta^{2'}_{\min})$, thus achieving complete control over the branching ratio.

Application: Coherent control of ultracold molecular collisions. As an example consider the coherent control of ultracold collisions of $^{17}O_2(X^3\Sigma)$ molecules in their ground electronic and rovibrational states ($v = N = 0$, where v is the vibrational quantum number and N is the quantum number related to the square of the rotational angular momentum $\hat{N}^2$). Cold and ultracold $O_2(X^3\Sigma) + O_2(X^3\Sigma)$ collisions were studied theoretically by several groups [42, 64–66] and have recently

been observed experimentally in a magnetically trapped oxygen gas at 800 mK [43]. We calculate the T-matrix elements for ultracold O_2 + O_2 collisions using a rigorous time-independent quantum scattering approach [42] as described in the Supplemental Material [67]. Due to their nonzero electron spin $S = 1$, $O_2(X^3\Sigma)$ molecules can occupy three different spin states $|M_S\rangle$ with $M_S = -1, 0$, and 1 (assuming $S = 1$ and neglecting the hyperfine structure for simplicity). An inelastic collision can change the spin projection of one or both molecules i.e., $|M_A, M_B\rangle_p \to |M'_A, M'_B\rangle_p$, where

$$|M_A, M_B\rangle_p = \frac{1}{\sqrt{2(1+\delta_{M_A M_B})}} \left[|M_A, M_B\rangle + p\,|M_B, M_A\rangle\right]. \tag{9}$$

These are internal states of the colliding molecules that have been identical particle symmetrized and that include the parity p of the state[42]. In this paper, we drop the index p, writing $|M_A, M_B\rangle$, when the calculated quantity (ICS or branching ratio) includes a sum on partial waves and then on the both parities.

More specifically, consider the nearly thermoneutral spin-exchange collisions $|0,0\rangle_p \leftrightarrow |-1,+1\rangle_p$, which can be used to generate entanglement [70] and quantum many-body phases in spinor Bose-Einstein condensates [71–73] and play an important role in ultracold atom-molecule and atom-ion chemistry [54, 74, 75]. At ultracold temperature, these flip-flop collisions occur in the s-wave regime for both the incident and final channels, thus forming an ideal testing ground for the application of the coherent control theory developed above. This regime could be achieved experimentally by evaporative or sympathetic cooling of trapped $^{17}O_2$ molecules [43, 76].

To coherently control the spin-exchange ICS to the final channels $|0,0\rangle$ and $|-1,+1\rangle$, consider three different kinds of coherent superpositions of the initial molecular spin states $|0,0\rangle_p$ and $|-1,+1\rangle_p$. In particular, *an entangled two-molecule superposition*

$$|\psi_E\rangle = \cos\eta\,|-1,+1\rangle_{p=\pm1} + \sin\eta e^{i\beta}\,|0,0\rangle_{p=+1} \tag{10}$$

cannot be represented as a direct product of the individual molecules's states. While this superposition is the simplest to consider from a theoretical perspective, and provides robust control (see below), it is challenging to prepare experimentally, as it requires entangling the internal states of the colliding molecules.

A non-entangled initial superposition has the form of a tensor product of two single-molecule superposition states $|\psi_A\rangle\,|\psi_B\rangle$, where

$$|\psi_A\rangle = N_2\left(\sqrt{\cos\eta}\,|-1\rangle + \sqrt{\sin\eta}e^{i\frac{\beta}{2}}\,|0\rangle\right) \tag{11}$$

$$|\psi_B\rangle = N_2\left(\sqrt{\sin\eta}e^{i\frac{\beta}{2}}\,|0\rangle + \sqrt{\cos\eta}\,|+1\rangle\right), \tag{12}$$

where $N_2 = (\sin\eta+\cos\eta)^{-1/2}$. For two identical bosonic molecules such as O_2, this initial state must be symmetrized to account for identical particle permutation symmetry [42] giving

$$|\psi_2^S\rangle = N_2^2\Big[\cos\eta\,|-1,+1\rangle_{p=\pm1} + \sin\eta e^{i\beta}\,|0,0\rangle_{p=+1} + \sqrt{\cos\eta\sin\eta}e^{i\frac{\beta}{2}}(|-1,0\rangle_{p=\pm1} + |0,+1\rangle_{p=\pm1})\Big]. \tag{13}$$

This initial state can be created in, e.g., merged beam experiments [77] by preparing coherent superpositions of internal states of the individual molecules prior to collision. In a similar way, we can prepare a *non-entangled three-state superposition*

$$|\psi_A\rangle = N_3\left[\sqrt{\cos\eta}(|-1\rangle + |+1\rangle) + \sqrt{\sin\eta}e^{i\frac{\beta}{2}}\,|0\rangle\right], \tag{14}$$

where $N_3 = (\sin\eta + 2\cos\eta)^{-1/2}$. After symmetrization, the initial wavefunction becomes

$$|\psi_3^S\rangle = N_3^2\Big[\cos\eta\,|-1,+1\rangle_{p=\pm1} + \sin\eta e^{i\beta}\,|0,0\rangle_{p=+1} + \sqrt{\cos\eta\sin\eta}e^{i\frac{\beta}{2}}(|-1,0\rangle_{p=\pm1} + |0,+1\rangle_{p=\pm1}) + \cos\eta(|-1,-1\rangle_{p=+1} + |+1,+1\rangle_{p=+1})\Big]. \tag{15}$$

A key difference between the entangled and non-entangled superpositions is the presence of the uncontrolled "*satellite terms*" [see Ref. [34]] $|-1,0\rangle_{p=\pm1}$ and $|0,+1\rangle_{p=\pm1}$ in $|\psi_2^S\rangle$ and $|-1,0\rangle_{p=\pm1}$, $|0,+1\rangle_{p=\pm1}$, $|-1,-1\rangle_{p=+1}$, and $|+1,+1\rangle_{p=+1}$ in $|\psi_3^S\rangle$.

Figure 1 shows the minimum and the maximum values of the ICS obtained with the initial superpositions $|\psi_E\rangle$, $|\psi_2^S\rangle$ and $|\psi_3^S\rangle$ to the final channels $|0,0\rangle$ and

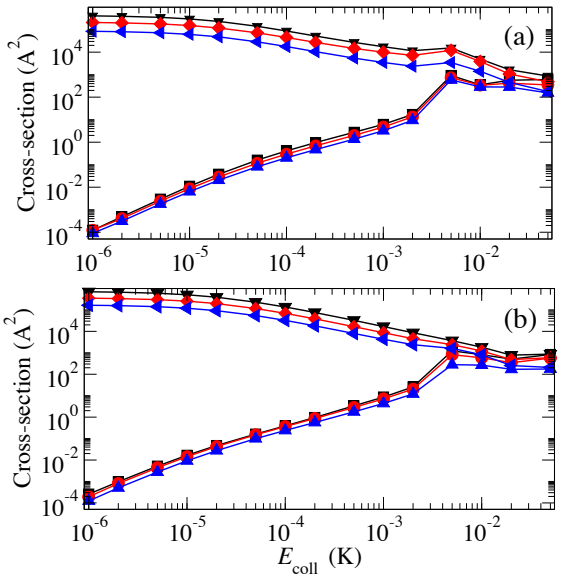

FIG. 1. Minimum (lower traces) and maximum (upper traces) ICSs from the initial superpositions $|\psi_E\rangle$ (black), $|\psi_2^S\rangle$ (red) and $|\psi_3^S\rangle$ (blue) to the final collisional channel (a) $|0,0\rangle$ and (b)$|-1,+1\rangle$.

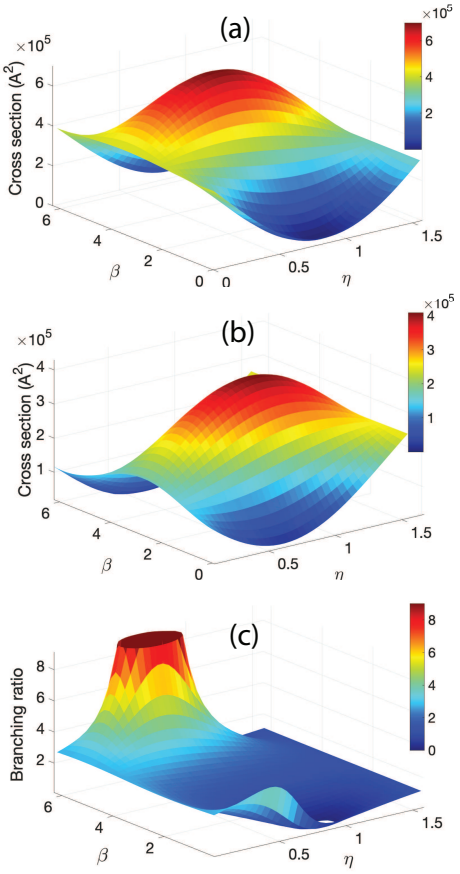

FIG. 2. Coherent control of the ICSs $\sigma_{s\to a'b'}$ for ultracold O_2 + O_2 collisions starting from the initial superposition $|\psi_2^S\rangle$ as a function of the superposition parameters η and β at a collision energy of 1 μK in the absence of external fields. The final states are $|-1,+1\rangle$ (a) and $|0,0\rangle$ (b). Panel (c) shows the branching ratio $\sigma_{s\to-1+1}/\sigma_{s\to00}$. While the values shown are limited to 8 to aid visibility, the maximal value of the branching ratio is 1.2×10^9.

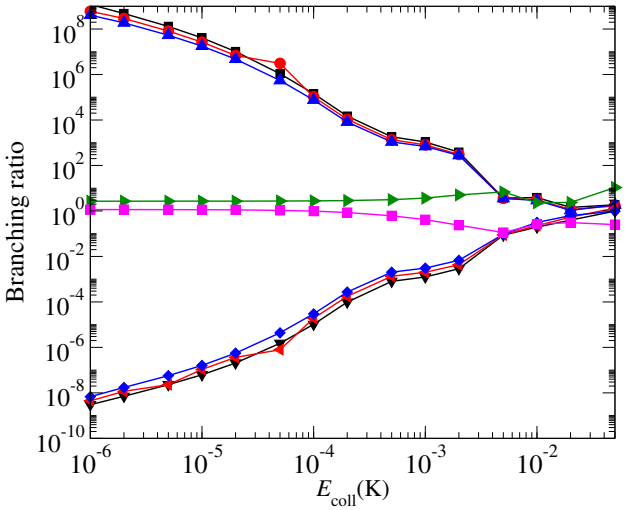

FIG. 3. Minimum (lower traces) and maximum (upper traces) of the branching ratio $\sigma_{s\to-1+1}/\sigma_{s\to00}$ for the initial superpositions $|\psi_E\rangle$ (black), $|\psi_2^S\rangle$ (red) and $|\psi_3^S\rangle$ (blue). The branching ratios in the absence of control are also shown as middle traces for the initial states $|-1,+1\rangle$ (triangles) and $|0,0\rangle$ (squares).

$|-1,+1\rangle$ as a function of collision energy $E_{\rm coll}$. The values for η and β were determined by the Eqs. (4), (5), (7), and (8). A remarkably wide, nine orders of magnitude range of control is observed for both final states. We further observe from Fig. 1 that the vast extent of coherent control in the s-wave regime is insensitive to whether the initial superposition is chosen to be entangled or non-entangled. The increase of $\sigma^{\rm min}$ with increasing collision energy observed in Fig. 1 is due to the growing contributions of the $\ell\geq2$ partial waves of the controllable term $\cos\eta\,|-1,+1\rangle_{p=+1}+\sin\eta e^{i\beta}\,|0,0\rangle_{p=+1}$, as well as by the spin exchange processes from the satellite terms, which change the value of the total angular momentum projection $M=M_A+M_B$, and thus require $\ell\geq2$ to occur. At $E_{\rm coll}<5$ mK, the s-wave to s-wave contribution to the ICS exceeds 99 % making the total ICS fully controllable and the contributions from the satellite terms negligible. In contrast, at collision energies above the height of the $\ell=2$ centrifugal barrier ($E_{\rm coll}>5$ mK) the non-s-wave contributions become dominant. As the contributions due to the satellite terms remain small compared to the d-wave contribution to the interference term, the ICSs depend only slightly on whether the initial superposition is entangled or non-entangled.

Figure 2 (a) and (b) shows the ICS for ultracold O_2 + O_2 collisions as a function of the initial superposition parameters η and β. In addition to the wide range of control for both the final spin exchange channels $|-1,+1\rangle$ and$|0,0\rangle$, we note that it is possible to tune the ICS in a continuous manner, reaching all intermediate values between zero and $\sigma_{\rm max}$ by varying the superposition angles η and β. The dependence of the ICS on η and β exhibits characteristic oscillations given by Eq. (3), which can be recognized as a signature of coherent control.

Finally, consider coherent control of the branching ratio $\sigma_{s\to-1+1}/\sigma_{s\to00}$, which is minimized when the ICS $\sigma_{s\to-1+1}$ is minimized and maximized when $\sigma_{s\to00}$ is minimized. At 1 μK, for example, the branching ratio can be varied from 10^{-9} to 10^8 demonstrating a truly outstanding range of control, spanning seventeen orders of magnitude! As a reference, the branching ratios in the absence of control are 2.69 and 1.15 for the initial states $|-1,+1\rangle$ and $|0,0\rangle$. Figure 2 (c) shows the branching ratio as a function of the initial superposition parameter. A sharp peak around the maximal value is observed. The range of control observed in Fig. 3 is much wider than in any previous study of coherent control [34, 36, 37], showing that the ultracold s-wave threshold regime provides optimal conditions for coherent control of quantum scattering dynamics. As in the case of the ICS, we observe a gradual loss of control as the collision energy is increased until control is completely lost outside of the s-wave regime at $E_{\rm coll}>5$ mK.

In conclusion, we have developed a general theory of quantum interference-based coherent control of ultra-

cold collisions, which allowed us to establish the possibility of complete coherent control over quantum scattering in the regime where only a single partial wave is involved in both the incident and final collision channels. We show that ultralow temperatures strongly enhance coherent control by favoring s-wave threshold scattering, and we determine the optimal parameters of the coherent superpositions required to maximize and minimize the ICS. The theory was applied to control ultracold spin-exchange collisions of oxygen molecules. We demonstrate vast control over both the ICS and their branching ratios in the s-wave threshold regime. These results demonstrate the possibility of using quantum interference as a powerful tool for controlling ultracold collision dynamics, which can be applied to a much wider range of molecular species (such as H_2) than dc field control. While ultracold collisions of rotationally excited molecules will generally be accompanied by rotational relaxation outside of the double s-wave regime, *ortho*-H_2+ *ortho*-H_2 collisions present a notable exception allowing for extensive coherent control. A natural extension of this work would be to explore coherent control of exothermic processes, which occur either directly in the multiple partial wave regime or via an isolated shape resonance [60, 78]. Our preliminary results show a large extent of control is possible in both cases.

This work was supported by the U.S. Air Force Office for Scientific Research (AFOSR) under Contract No. FA9550-19-1-0312. SciNet computational facilities are gratefully acknowledged.

[1] J. L. Bohn, A. M. Rey, and J. Ye, Cold molecules: Progress in quantum engineering of chemistry and quantum matter, Science **357**, 1002 (2017).
[2] L. R. Liu, J. D. Hood, Y. Yu, J. T. Zhang, N. R. Hutzler, T. Rosenband, and K. K. Ni, Building one molecule from a reservoir of two atoms, Science **360**, 900 (2018).
[3] M. A. Norcia, A. W. Young, and A. M. Kaufman, Microscopic control and detection of ultracold strontium in optical-tweezer arrays, Phys. Rev. X **8**, 041054 (2018).
[4] A. Cooper, J. P. Covey, I. S. Madjarov, S. G. Porsev, M. S. Safronova, and M. Endres, Alkaline-earth atoms in optical tweezers, Phys. Rev. X **8**, 041055 (2018).
[5] I. Bloch, J. Dalibard, and W. Zwerger, Many-body physics with ultracold gases, Rev. Mod. Phys. **80**, 885 (2008).
[6] C. Gross and I. Bloch, Quantum simulations with ultracold atoms in optical lattices, Science **357**, 995 (2017).
[7] L. D. Carr, D. DeMille, R. V. Krems, and J. Ye, Cold and ultracold molecules: science, technology and applications, New J. Phys **11**, 055049 (2009).
[8] R. V. Krems, Cold controlled chemistry, Phys. Chem. Chem. Phys. **10**, 4079 (2008).
[9] N. Balakrishnan, Perspective: Ultracold molecules and the dawn of cold controlled chemistry, J. Chem. Phys. **145**, 150901 (2016).
[10] C. Chin, R. Grimm, P. Julienne, and E. Tiesinga, Feshbach resonances in ultracold gases, Rev. Mod. Phys. **82**, 1225 (2010).
[11] W. C. Stwalley, Stability of spin-aligned hydrogen at low temperatures and high magnetic fields: New field-dependent scattering resonances and predissociations, Phys. Rev. Lett. **37**, 1628 (1976).
[12] E. Tiesinga, B. J. Verhaar, and H. T. C. Stoof, Threshold and resonance phenomena in ultracold ground-state collisions, Phys. Rev. A **47**, 4114 (1993).
[13] P. O. Fedichev, Y. Kagan, G. V. Shlyapnikov, and J. T. M. Walraven, Influence of nearly resonant light on the scattering length in low-temperature atomic gases, Phys. Rev. Lett. **77**, 2913 (1996).
[14] A. Devolder, E. Luc-Koenig, O. Atabek, M. Desouter-Lecomte, and O. Dulieu, Laser-assisted self-induced feshbach resonance for controlling heteronuclear quantum gas mixtures, Phys. Rev. A **100**, 052703 (2019).
[15] T. V. Tscherbul, T. Calarco, I. Lesanovsky, R. V. Krems, A. Dalgarno, and J. Schmiedmayer, rf-field-induced Feshbach resonances, Phys. Rev. A **81**, 050701 (2010).
[16] A. V. Avdeenkov and J. L. Bohn, Linking ultracold polar molecules, Phys. Rev. Lett. **90**, 043006 (2003).
[17] T. V. Tscherbul and R. V. Krems, Tuning bimolecular chemical reactions by electric fields, Phys. Rev. Lett. **115**, 023201 (2015).
[18] V. Sanchez-Villicana, S. D. Gensemer, K. Y. N. Tan, A. Kumarakrishnan, T. P. Dinneen, W. Süptitz, and P. L. Gould, Suppression of ultracold ground-state hyperfine-changing collisions with laser light, Phys. Rev. Lett. **74**, 4619 (1995).
[19] A. V. Avdeenkov, M. Kajita, and J. L. Bohn, Suppression of inelastic collisions of polar $^1\Sigma$ state molecules in an electrostatic field, Phys. Rev. A **73**, 022707 (2006).
[20] S. V. Alyabyshev, T. V. Tscherbul, and R. V. Krems, Microwave-laser-field modification of molecular collisions at low temperatures, Phys. Rev. A **79**, 060703 (2009).
[21] G. Quéméner and J. L. Bohn, Shielding $^2\Sigma$ ultracold dipolar molecular collisions with electric fields, Phys. Rev. A **93**, 012704 (2016).
[22] T. Karman and J. M. Hutson, Microwave shielding of ultracold polar molecules, Phys. Rev. Lett. **121**, 163401 (2018).
[23] L. Lassablière and G. Quéméner, Controlling the scattering length of ultracold dipolar molecules, Phys. Rev. Lett. **121**, 163402 (2018).
[24] T. Xie, M. Lepers, R. Vexiau, A. Orban, O. Dulieu, and N. Bouloufa-Maafa, Optical shielding of destructive chemical reactions between ultracold ground-state NaRb molecules, Phys. Rev. Lett. **125**, 153202 (2020).
[25] E. Abrahamsson, T. V. Tscherbul, and R. V. Krems, Inelastic collisions of cold polar molecules in nonparallel electric and magnetic fields, J. Chem. Phys. **127**, 044302 (2007).
[26] T. V. Tscherbul and R. V. Krems, Controlling electronic spin relaxation of cold molecules with electric fields, Phys. Rev. Lett. **97**, 083201 (2006).
[27] Z. Li, S. V. Alyabyshev, and R. V. Krems, Ultracold inelastic collisions in two dimensions, Phys. Rev. Lett. **100**, 073202 (2008).
[28] Z. Li and R. V. Krems, Inelastic collisions in an ul-

tracold quasi-two-dimensional gas, Phys. Rev. A **79**, 050701 (2009).
[29] M. H. G. de Miranda, A. Chotia, B. Neyenhuis, D. Wang, G. Quéméner, S. Ospelkaus, J. L. Bohn, J. Ye, and D. S. Jin, Controlling the quantum stereodynamics of ultracold bimolecular reactions, Nat. Phys. **7**, 502 (2011).
[30] Z. Ren, L. Che, M. Qiu, X. Wang, W. Dong, D. Dai, X. Wang, X. Yang, Z. Sun, B. Fu, S.-Y. Lee, X. Xu, and D. H. Zhang, Probing the resonance potential in the F atom reaction with hydrogen deuteride with spectroscopic accuracy, Proc. Natl. Acad. Sci. USA **105**, 12662 (2008).
[31] M. Tizniti, S. D. L. Picard, F. Lique, C. Berteloite, A. Canosa, M. H. Alexander, and I. R. Sims, The rate of the F + H_2 reaction at very low temperatures, Nat. Chem. **6**, 141 (2014).
[32] D. D. Fazio, V. Aquilanti, and S. Cavalli, Benchmark quantum kinetics at low temperatures toward absolute zero and role of entrance channel wells on tunneling, virtual states, and resonances: The F + HD reaction, J. Phys. Chem. A **124**, 12 (2020).
[33] M. S. Safronova, D. Budker, D. DeMille, D. F. J. Kimball, A. Derevianko, and C. W. Clark, Search for new physics with atoms and molecules, Rev. Mod. Phys. **90**, 025008 (2018).
[34] M. Shapiro and P. Brumer, *Quantum control of Molecular Processes* (Wiley-VCH, 2012).
[35] T. Scholak and P. Brumer, An approach to 'quantumness' in coherent controls, Adv. Chem. Phys. **162**, 39 (2017).
[36] J. J. Omiste, J. Floß, and P. Brumer, Coherent control of Penning and associative ionization: Insights from symmetries, Phys. Rev. Lett. **121**, 163405 (2018).
[37] A. Devolder, T. V. Tscherbul, and P. Brumer, Coherent control of reactive scattering at low temperatures: Signatures of quantum interference in the differential cross sections for F + H_2 and F + HD, Phys. Rev. A **102**, 031303 (2020).
[38] M. Shapiro and P. Brumer, Coherent control of collisional events: Bimolecular reactive scattering, Phys. Rev. Lett. **77**, 2574 (1996).
[39] J. Gong, M. Shapiro, and P. Brumer, Entanglement-assisted coherent control in nonreactive diatom–diatom scattering, J. Chem. Phys. **118**, 2626 (2003).
[40] P. Brumer, A. Abrashkevich, and M. Shapiro, Laboratory conditions in the coherent control of reactive scattering, Faraday Discuss. **113**, 291 (1999).
[41] F. Herrera, Magnetic-field-induced interference of scattering states in ultracold collisions, Phys. Rev. A **78**, 054702 (2008).
[42] T. V. Tscherbul, Y. V. Suleimanov, V. Aquilanti, and R. V. Krems, Magnetic field modification of ultracold molecule–molecule collisions, New J. Phys. **11**, 055021 (2009).
[43] Y. Segev, M. Pitzer, M. Karpov, N. Akerman, J. Narevicius, and E. Narevicius, Collisions between cold molecules in a superconducting magnetic trap, Nature **572**, 189 (2019).
[44] H. R. Sadeghpour, J. L. Bohn, M. Cavagnero, B. D. Esry, I. I. Fabrikani, J. H. Macek, and A. R. P. Rau, Collisions near threshold in atomic and molecular physics, J. Phys. B **33**, R39 (2000).
[45] R. V. Krems, Molecules near absolute zero and external field control of atomic and molecular dynamics, Int. Rev. Phys. Chem. **24**, 99 (2005).
[46] A. Volpi and J. L. Bohn, Magnetic-field effects in ultracold molecular collisions, Phys. Rev. A **65**, 052712 (2002).
[47] R. V. Krems and A. Dalgarno, Threshold laws for collisional reorientation of electronic angular momentum, Phys. Rev. A **67**, 050704 (2003).
[48] K. A. Safinya, J. F. Delpech, F. Gounand, W. Sandner, and T. F. Gallagher, Resonant Rydberg-Atom-Rydberg-Atom collisions, Phys. Rev. Lett. **47**, 405 (1981).
[49] R. A. D. S. Zanon, K. M. F. Magalhaes, A. L. de Oliveira, and L. G. Marcassa, Time-resolved study of energy-transfer collisions in a sample of cold rubidium atoms, Phys. Rev. A **65**, 023405 (2002).
[50] I. I. Ryabtsev, D. B. Tretyakov, I. I. Beterov, and V. M. Entin, Observation of the Stark-tuned Förster resonance between two Rydberg atoms, Phys. Rev. Lett. **104**, 073003 (2010).
[51] J. Nipper, J. B. Balewski, A. Krupp, B. Butscher, R. Low, and T. Pfau, Highly resolved measurements of Stark-tuned forster resonances between Rydberg atoms, Phys. Rev. Lett. **108**, 113001 (2012).
[52] S. Ravets, H. Labuhn, D. Barredo, L. Béguin, T. Lahaye, and A. Browaeys, Coherent dipole–dipole coupling between two single Rydberg atoms at an electrically-tuned Förster resonance, Nat. Phys. **10**, 914 (2014).
[53] A. L. Win, W. D. Williams, T. J. Carroll, and C. I. Sukenik, Catalysis of Stark-tuned interactions between ultracold Rydberg atoms, Phys. Rev. Lett. **108**, 032703 (2012).
[54] J. Rui, H. Yang, L. Liu, D.-C. Zhang, Y.-X. Liu, J. Nan, Y.-A. Chen, B. Zhao, and J.-W. Pan, Controlled state-to-state atom-exchange reaction in an ultracold atom–dimer mixture, Nat. Phys. **13**, 699 (2017).
[55] M. Bouledroua, A. Dalgarno, and R. Côté, Diffusion and excitation transfer of excited alkali atoms, Phys. Rev. A **65**, 012701 (2001).
[56] R. Côté and A. Dalgarno, Ultracold atom-ion collisions, Phys. Rev. A **62**, 012709 (2000).
[57] E. Bodo, P. Zhang, and A. Dalgarno, Ultra-cold ion–atom collisions: near resonant charge exchange, New J. Phys. **10**, 033024 (2008).
[58] P. Zhang, A. Dalgarno, and R. Côté, Scattering of Yb and Yb^+, Phys. Rev. A **80**, 030703 (2009).
[59] W. E. Perreault, N. Mukherjee, and R. N. Zare, Quantum control of molecular collisions at 1 Kelvin, Science **358**, 356 (2017).
[60] P. G. Jambrina, J. F. E. Croft, H. Guo, M. Brouard, N. Balakrishnan, and F. J. Aoiz, Stereodynamical control of a quantum scattering resonance in cold molecular collisions, Phys. Rev. Lett. **123**, 043401 (2019).
[61] M. Morita, Q. Yao, C. Xie, H. Guo, and N. Balakrishnan, Stereodynamic control of overlapping resonances in cold molecular collisions, Phys. Rev. Research **2**, 032018 (2020).
[62] M. Morita and N. Balakrishnan, Stereodynamics of ultracold rotationally inelastic collisions, J. Chem. Phys. **153**, 184307 (2020).
[63] E. Frishman, M. Shapiro, and P. Brumer, Coherent enhancement and suppression of reactive scattering and tunneling, J. Chem. Phys. **110**, 9 (1998).
[64] J. Pérez-Rios, M. Bartolomei, J. Campos-Martinez, M. I. Hernandez, and R. Hernandez-Lamoneda,

Quantum-mechanical study of the collision dynamics of $O_2 + O_2$ on a new ab initio potential energy surface, J. Phys. Chem. A **113**, 14952 (2009).
[65] A. V. Avdeenkov and J. L. Bohn, Ultracold collisions of oxygen molecules, Phys. Rev. A **64**, 052703 (2001).
[66] G. Guillon, M. Lepers, and P. Honvault, Quantum dynamics of ^{17}O in collision with ortho- and para-$^{17}O^{17}O$, Phys. Rev. A **102**, 012810 (2020).
[67] See Supplemental Material at [URL], which includes Refs. [68, 69] for details of quantum scattering calculations and convergence tests.
[68] V. Aquilanti, D. Ascenzi, M. Bartolomei, D. Cappelletti, S. Cavalli, M. d. C. Vitores, and F. Pirani, Quantum interference scattering of aligned molecules: Bonding in O_4 and role of spin coupling, Phys. Rev. Lett. **82**, 69 (1999).
[69] V. Aquilanti, D. Ascenzi, M. Bartolomei, D. Cappelletti, S. Cavalli, M. d. C. Vitores, and F. Pirani, Molecular beam scattering of aligned oxygen molecules. The nature of the bond in the O_2-O_2 dimer, J. Am. Chem. Soc. **121**, 10794 (1999).
[70] L.-M. Duan, J. I. Cirac, and P. Zoller, Quantum entanglement in spinor Bose-Einstein condensates, Phys. Rev. A **65**, 033619 (2002).
[71] M.-S. Chang, Q. Qin, W. Zhang, L. You, and M. S. Chapman, Coherent spinor dynamics in a spin-1 Bose condensate, Nat. Phys. **1**, 111 (2005).
[72] Y. Kawaguchi and M. Ueda, Spinor Bose-Einstein condensates, Phys. Rep. **520**, 253 (2012).
[73] D. M. Stamper-Kurn and M. Ueda, Spinor Bose gases: Symmetries, magnetism, and quantum dynamics, Rev. Mod. Phys. **85**, 1191 (2013).
[74] Y.-X. Liu, J. Nan, D.-C. Zhang, L. Liu, H. Yang, J. Rui, B. Zhao, and J.-W. Pan, Observation of a threshold behavior in an ultracold endothermic atom-exchange process involving feshbach molecules, Phys. Rev. A **100**, 032706 (2019).
[75] T. Sikorsky, M. Morita, Z. Meir, A. A. Buchachenko, R. Ben-shlomi, N. Akerman, E. Narevicius, T. V. Tscherbul, and R. Ozeri, Phase locking between different partial waves in atom-ion spin-exchange collisions, Phys. Rev. Lett. **121**, 173402 (2018).
[76] N. Akerman, M. Karpov, Y. Segev, N. Bibelnik, J. Narevicius, and E. Narevicius, Trapping of molecular oxygen together with lithium atoms, Phys. Rev. Lett. **119**, 073204 (2017).
[77] A. B. Henson, S. Gerstein, Y. Shagam, J. Narevicius, and E. Narevicius, Observation of resonances in Penning ionization reactions at sub-Kelvin temperatures in merged beams, Science **338**, 234 (2012).
[78] V. Zeman, M. Shapiro, and P. Brumer, Coherent control of resonance-mediated reactions: F + HD, Phys. Rev. Lett. **92**, 133204 (2004).